Macromolecules **1986,** *19,* 1317-1324

(20) Crist, B. *J. Polym. Sci., Polym. Sci., Polym. Phys. Ed.* **1973,** *11,* 635.
(21) Hosemann, R.; Bredin, O. W. *Chem. Techn. Cell.* **1980,** *14,* 583.
(22) Vonk, C. J.; Kortleve, G. *Kolloid Z. Z. Polym.* **1967,** *220,* 19.
(23) Vonk, C. *J. Appl. Crystallogr.* **1975,** *8,* 340.
(24) Demus, D.; Richter, L. "LC Textures"; VEB Fachbuchverlag: Leipzig, 1980.
(25) Shilov, V. V.; Tsukruk, V. V.; Bliznyuk, V. N.; Lipatov, Yu. S. *Polymer* **1982,** *23,* 484.
(26) Lipatov, Yu. S.; Tsukruk, V. V.; Shilov, V. V. *Polym. Commun.* **1983,** *24,* 75.
(27) Tsukruk, V. V.; Shilov, V. V.; Lipatov, Yu. S. *Eur. Polym. J.* **1983,** *19,* 199.
(28) Lipatov, Yu. S.; Shilov, V. V.; Tsukruk, V. V. *Ukr. Phys. J.* **1983,** *28,* 543.
(29) Plate, N. A.; Shibaev, V. P. "Comb-like Polymers and Liquid Crystals"; Nauka: Moscow, 1980 (in Russian).
(30) Blumstein, A.; Klug, S.; de Vries, A. *Polym. Prepr. (Am. Chem. Soc.-Div. Polym. Chem.* **1977,** *17,* 1.
(31) Tsukruk, V. V.; Shilov, V. V.; Lipatov, Yu. S.; Konstantinov, I. I.; Amerik, Yu. B. *Acta Polym.* **1982,** *33,* 63.
(32) Strobl, G. R.; Schneider, M. *J. Polym. Sci., Polym. Phys. Ed.* **1980,** *18,* 1343.
(33) Hosemann, R.; Bagchi, S. "Direct Analysis Diffraction by Matter"; North-Holland: Amsterdam, 1962.
(34) Tsukruk, V. V.; Shilov, V. V.; Lipatov, Yu. S. *Crystallogr.*, in press.
(35) Vonk, C. J. *J. Appl. Crystallogr.* **1973,** *6,* 81.
(36) Hashimoto, T.; Shibayama, M.; Kawai, N. *Macromolecules* **1980,** *13,* 1237.
(37) Roe, R. J.; Fishkis, M.; Chang, J. S. *Macromolecules* **1981,** *14,* 1091.
(38) Lipatov, Yu. S. "Interphase Phenomena in Polymers"; Naukova Dumka: Kiev, USSR, 1980 (in Russian).
(39) Bonart, R.; Muller, E. H. *J. Macromol. Sci. Phys.* **1974,** *10,* 345.
(40) Koberstein, L. Stein, R. *J. Polym. Sci., Polym. Phys. Ed.* **1983,** *21,* 1439.
(41) Tsukruk, V. V.; Shilov, V. V.; Lipatov, Yu. S. *Makromol. Chem.* **1982,** *183,* 2009.
(42) Cser, F. In "Abstracts, Fourth Conference on Liquid Crystals", Tbilisi, 1981; Nauka: Moscow, 1981; Vol. 2, p 190.
(43) Davidov, D.; Safiniy, C. R.; Kaplan, M.; Dana, S. S.; Litster, J. D. *Phys. Rev.* **1979,** *B19,* 1657.
(44) Safiniy, C. R.; Kaplan, M.; Als-Neisen, J.; Birgenau, R. J.; Davidov, D.; Litster, Y. D. *Phys. Rev. B: Condens. Matter* **1980,** *B21,* 4149.
(45) Lipatov, Yu. S.; Tsukruk, V. V.; Shilov, V. V. *J. Macromol. Sci., Rev. Macromol. Chem. Phys.* **1984,** *24,* 173.
(46) Vainstein, B. K. "X-ray Diffraction on Chain Molecules"; Nauka: Moscow, 1963 (in Russian).
(47) de Gennes, P. "Concepts in Scaling in Polymer Physics"; Cornell University Press: Ithaca, NY, 1979.
(48) Tsukruk, V.; Shilov, V.; Lipatov, Yu. *J. Polym. Sci., Polym. Phys. Ed.* **1984,** *22,* 41.

From Plastic-Crystal Paraffins to Liquid-Crystal Polyethylene: Continuity of the Mesophase in Hydrocarbons

Goran Ungar

H. H. Wills Physics Laboratory, Bristol BS8 1TL, England, and Rudjer Bošković Institute, POB 1016, Zagreb, Yugoslavia.

Received December 4, 1985

ABSTRACT: The relationship is explored between the plastic "rotator" phase (RP), which occurs in *n*-alkanes up to C_{40}, and the "liquid-crystalline" high-pressure hexagonal phase (HPHP) in polyethylene. The radiation-induced hexagonal phase (RIHP) of polyethylene, which is intermediate between the two, has been shown in a previous study to behave with increasing pressure essentially like HPHP. In this work a link is demonstrated between RP and RIHP through a study of paraffin C_{11}, binary paraffins C_{23}–C_{25} and C_{36}–C_{40}, as well as irradiated polyethylene by Fourier-transform infrared spectroscopy. Absence of GG defects and presence of GTG* kinks was confirmed in both RP and RIHP. A smooth continuity was established between the two phases by the defect concentration criterion. More evidence for such continuity is provided by a systematic comparison of published pressure–temperature diagrams for paraffins and polyethylenes. Moreover, the available data for high-temperature forms in related systems (high-modulus polyethylene fibers, cycloalkanes, and substituted *n*-alkanes) all suggest that a single master relation between the degree of order and variables such as temperature and chain stem length can, to a good approximation, describe the qualitative behavior of the wide range of hexagonal or pseudohexagonal phases in hydrocarbon chain systems.

Introduction

n-Alkanes up to tetracontane (C_{40}) undergo on heating a strong first-order transition a few degrees below the melting point into the so-called rotator phase (RP). This has been extensively studied both experimentally[1-12] and theoretically[13-16] partly because of the importance of RP in understanding the order and mobility in chain molecular systems and partly because of its direct relevance to phase behavior in phospholipid layers[17] and, recently, in Langmuir–Blodgett films.[18]

Quite independently of the research on paraffins, studies were performed on the high-pressure hexagonal phase (HPHP) in polyethylene.[19-26] The two phenomena have mostly been treated separately and have generally been considered to be qualitatively different.

The distinction between RP and HPHP originates from the following. The earlier studies of RP were mainly performed on relatively short paraffins, around 20 C atoms long. X-ray diffraction[1] and Raman spectroscopy[2] indicated that chains retain their all-trans conformation in RP, the disorder being accounted for by hindered rotation around the chain axis together with a degree of translational motion.[12] The nearest description of RP would thus be that of a plastic-crystal state. In contrast, HPHP is considered to contain a large proportion of gauche bonds. Largely on the basis of the similarity of Raman spectra of HPHP and the melt,[23] it was concluded that the chain conformation in HPHP does not differ significantly from that in the melt. Further, while the ratio of entropies of the orthorhombic–hexagonal (o–h) and hexagonal–melt (h–m) transitions in paraffins ranges from $(s_h - s_o)/(s_m - s_h) = 0.3–0.6$,[27] in polyethylene at high pressures this ratio is around 3.[22] HPHP has accordingly been described as a liquid crystal[28] or a "condis" (conformationally disordered) crystal form.[29]

The different behavior of RP and HPHP with increasing pressure has been taken as a further distinguishing feature: while RP disappears with increasing pressure, HPHP is

0024-9297/86/2219-1317$01.50/0

stable only at high pressures, the triple point being at about 4 kbar.[22] From the Clapeyron equation two inequalities for RP and HPHP were thus derived,[30] relating changes in specific volumes (v) and entropies (s)

Paraffins (h = RP)

$$\frac{s_h - s_o}{s_m - s_h} < \frac{v_h - v_o}{v_m - v_h} \tag{1a}$$

Polyethylene (h = HPHP)

$$\frac{s_h - s_o}{s_m - s_h} > \frac{v_h - v_o}{v_m - v_h} \tag{1b}$$

In view of these relationships RP has been termed a "high-volume", and HPHP a "high-entropy" phase.[30]

In this paper evidence is presented in favor of a unified description of RP, HPHP, and related mesophases[56] in polyethylenes, cycloalkanes, and end-substituted hydrocarbons. More specifically, it is shown that the increasing temperature at which the hexagonal phase is stable in progressively longer paraffins results in increasing disorder which is, in the main, continuous and which ties up well with the observed features of HPHP. Bridging the gap between RP and HPHP, the radiation-induced hexagonal phase (RIHP) in polyethylene helps in establishing the continuity. The evidence stems from already published data, as well as from new, mainly IR, spectroscopic experiments. Additional X-ray diffraction evidence will be presented elsewhere.[31]

Evidence for Continuity from Pressure–Temperature Behavior

A fair number of pressure–temperature (p–T) diagrams of n-alkanes and polyethylene has been published over the years. Figure 1 is a collection of most of them, placed on the same scale. The figure also includes diagrams for two irradiated polyethylenes as well as that for 1,20-eicosanedioic acid, $HOOC(CH_2)_{18}COOH$. The point to note in Figure 1 is that the convergence of the orthorhombic–hexagonal and hexagonal–melt phase boundaries, i.e., $(dT_{o-h}/dp)-(dT_{h-m}/dp)$, becomes progressively smaller with increasing chain length. At a length of about 40 C atoms or somewhat higher the two lines become parallel, thus satisfying the condition

$$(s_h - s_o)/(s_m - s_h) = (v_h - v_o)/(v_m - v_h)$$

By extrapolation to still longer chains it is only to be expected that $T_{o-h}(p)$ and $T_{h-m}(p)$ would start diverging as in polyethylene. Thus p–T diagrams give *no* evidence of a qualitative difference between RP and HPHP but rather suggest continuity between the two.

The main remaining problem, however, is that in the large gap between paraffin C_{40} and extended-chain polyethylene the mesophase cannot normally be observed as the o–h transition is intercepted by melting. Nevertheless, at the melting point the free enthalpy g_h of the hexagonal phase is not much higher than g_o and g_m. Thus by preferentially increasing one or both of the latter free enthalpies the hexagonal phase can be made stable within the temperature gap range 110–230 °C. For example, in the case of C_{20}-dicarboxylic acid (C_{20}DCA) an increase in g_m is achieved by reducing the configurational entropy of the melt through intermolecular hydrogen bonding.[26] In irradiated polyethylene a similar effect is achieved through covalent cross-linking, but in addition g_o is increased through the introduction of lattice defects.[37] As seen in Figure 1, a sufficiently high irradiation dose (500 Mrad) makes RIHP stable even at atmospheric pressure. According to criterion 1 the hexagonal phases in both C_{20}DCA and in irradiated polyethylene would be designated as "high-entropy" phases. It may be remarked that the nematic phase in most cases is also of this type; i.e., it is stabilized by pressure.[38,39]

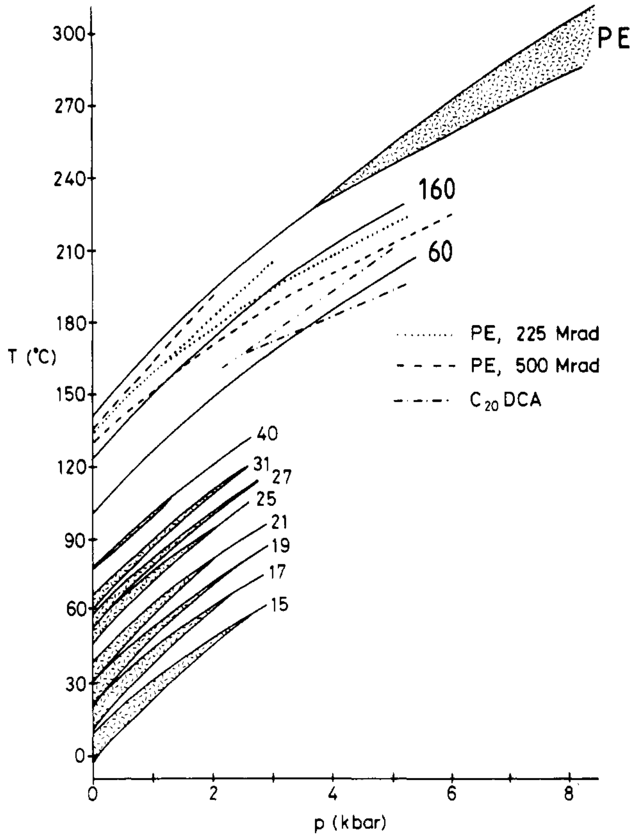

Figure 1. Pressure–temperature diagrams of n-alkanes and polyethylene. Shaded areas indicate regions of stability of the mesophase ("hexagonal" phase). Data for alkanes C_{15}, C_{17}, C_{19}, C_{21}, C_{25}, C_{27}, and C_{31} are from ref 32, for C_{40} from ref 33, for C_{60} and C_{160} from ref 34, and for polyethylene from ref 22. Diagrams for irradiated polyethylene (225 and 500 Mrad) are included[35] as well as that for 1,20-eicosanedioic acid, C_{20}DCA.[36]

The fact that RIHP can be observed at atmospheric pressure allows the chain conformation to be conveniently studied by infrared spectroscopy. IR results on RIHP and RP will be described later on.

A comment on the p–T behavior of paraffin C_{40} is in place at this point. Whereas all other diagrams in Figure 1 were determined by thermal analysis, the one for C_{40} was derived optically.[33] The two transitions T_{o-h} and T_{h-m} were so close (only 0.3 K difference at 1 bar) that they could not be resolved by thermal analysis. Raman spectra were recorded at temperatures between T_{o-h} and T_{h-m} at different pressures,[33] and due to their close resemblance to melt spectra it was concluded that the intermediate phase was not of the RP type but rather of the HPHP type. However, this conclusion is open to question since the close proximity of T_{o-h} to the melting point means that at any temperature between the two transitions a significant portion of the material is molten. It is thus likely that the Raman spectra represent a mixture of the intermediate phase and the melt, rather than the pure intermediate phase. In view of the fact that extrapolation of T_{o-h} and T_{h-m} values from shorter paraffins predicts a rotator phase in C_{40} stable over a 0.8 K interval at 1 bar,[27] it seems reasonable to treat the intermediate phase observed in C_{40} as a continuation of RP of the shorter chain homologues. Additional support for this proposal comes from our IR results on a C_{36}–C_{40} paraffin mixture, which show the high-temperature phase falling in line with other rotator phases (see further below).

Table I
Thermodynamic Data for Alkane C_{21}

	value	meas at temp, K	source	value at T_1 = 308 K
$s_h - s_o$			this work[a]	0.180 J/gK
$s_m - s_h$			this work[a]	0.513 J/gK
v_o			this work[b] and ref 6	1.085 cm^3/g
v_h			this work[b] and ref 6	1.139 cm^3/g
v_m	293.2	1.264	ref 42, Figure 4	1.280 cm^3/g[c]
$c_{p,o}$	298	1.85	this work[d]	1.85 J/g·K
$c_{p,h}$			this work[d]	5.2 J/g·K
$c_{p,m}$	298	2.25	ref 43[e]	2.25 J/g·K
α_o	298	0.51×10^{-3} K^{-1}	this work and ref 6	0.51×10^{-3} K^{-1}
α_h			this work and ref 6	1.75×10^{-3} K^{-1}
α_m	293–343	0.84×10^{-3} K^{-1}	ref 42, Figure 4	0.84×10^{-3} K^{-1}

[a] DSC measurement. *n*-Heneicosane was purchased from Sigma Chemicals and further purified by recrystallization from acetone/tetrachlorethylene. [b] From X-ray unit cell parameters obtained from continuous-temperature scans using a Guinier–Lenne camera. [c] Assuming constant thermal expansivity given in this table. [d] DSC measurement in c_p mode, 15-mg sample, heating rate of 0.62 K/min, sapphire standard. [e] From $c_{p,m}$ values for odd-numbered *n*-alkanes extrapolated to $n = 21$ carbon atoms.

The case of C_{20}DCA (Figure 1) illustrates most clearly that the change from convergence to divergence of $T_{o-h}(p)$ and $T_{h-m}(p)$ is an effect of increasing temperature: in a paraffin of the same chain length, i.e., around 20 C atoms, RP is stable at around 30 °C at 1 bar and it is "convergent"; for C_{20}DCA an extrapolation to atmospheric pressure gives a "virtual" hexagonal phase in the range of 130 °C, which would be "divergent" in the sense that $(\mathrm{d}T_{h-m}/\mathrm{d}p)_{1\,\mathrm{bar}} > (\mathrm{d}T_{o-h}/\mathrm{d}p)_{1\,\mathrm{bar}}$.

Thermodynamic data for individual paraffins, notably the high heat capacity of RP, in fact predict such a continuous change with temperature from convergence to divergence of $T_{o-h}(p)$ and $T_{h-m}(p)$ at $p = 1$ bar. On the basis of the available experimental data for paraffin C_{21}, it is easily shown that the inequality 1a (condition for convergence) has a tendency to change into inequality 1b with increasing temperature. Let

$$\left(\frac{s_h - s_o}{s_m - s_h}\right)_{1\,\mathrm{bar}} = r$$

$$\left(\frac{v_h - v_o}{v_m - v_n}\right)_{1\,\mathrm{bar}} = u$$

Differentiate

$$\frac{\mathrm{d}r}{\mathrm{d}T} = \frac{c_{p,m} - c_{p,h}}{T(s_m - s_h)}\left(\frac{c_{p,h} - c_{p,o}}{c_{p,m} - c_{p,h}} - \frac{s_h - s_o}{s_m - s_h}\right) \tag{2a}$$

$$\frac{\mathrm{d}u}{\mathrm{d}T} = \frac{v_m\alpha_m - v_h\alpha_h}{v_m - v_h}\left(\frac{v_h\alpha_h - v_o\alpha_o}{v_m\alpha_m - v_h\alpha_h} - \frac{v_h - v_o}{v_m - v_h}\right) \tag{2b}$$

where c_p's denote heat capacities and α's thermal expansivities. For r or u to be independent of temperature requires that the expression in brackets by zero. However, since both c_p and α of the rotator phase by far exceed those of the melt,[10,40] both r and u will increase steeply with temperature, thus bringing the hexagonal phase closer to the melt both in entropy and in volume. It should be noted that such behavior is not unique to RP: thermal expansivity of HPHP was found by dilatometry to be higher than that of the melt.[20] Similarly, exceptionally high lateral linear expansivities were found by X-ray diffraction in RIHP[31] and in the hexagonal phase of constrained high-modulus polyethylene fibers.[41] Unfortunately, corresponding c_p data are not available.

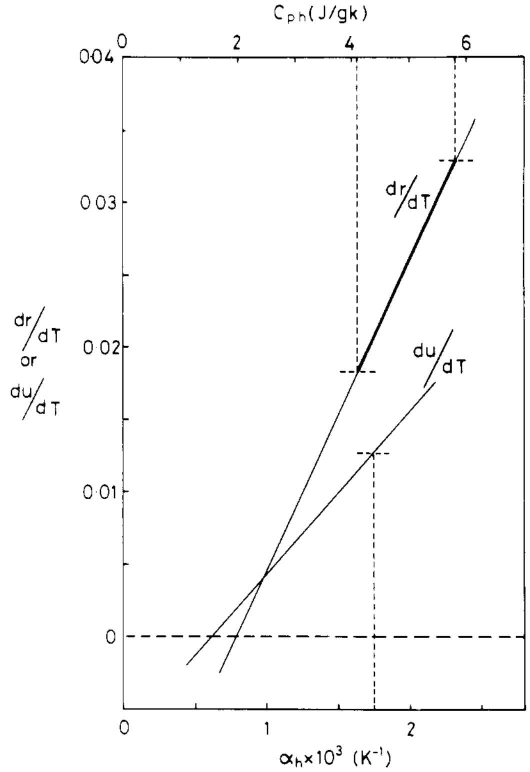

Figure 2. Rate of increase in relative entropy and volume of the rotator phase with temperature, $\mathrm{d}r/\mathrm{d}T$ and $\mathrm{d}u/\mathrm{d}T$, as functions of the heat capacity, $c_{p,h}$ and thermal expansivity, α_h, respectively, according to eq 2. Thermodynamic values for paraffin C_{21} at 308 K are used (Table I). The range of $c_{p,h}$ measured in the FCO rotator phase of 3/1 C_{21}–C_{23} binary paraffin[10] is indicated.

Further, by taking paraffin C_{21} as an example, it can be readily shown that $\mathrm{d}r/\mathrm{d}t > \mathrm{d}u/\mathrm{d}T$. All necessary quantities are given in Table I for an arbitrarily chosen temperature $T_1 = 308$ K, at which RP is stable. Measurements on paraffins show[10,40] that the heat capacity of RP varies significantly with temperature: e.g., in a single system, a 3/1 mixture of C_{21} and C_{23}, $c_{p,h}$ was found to vary between 4.1 and 5.8 J/g·K over the 16 K interval of stability of the FCO rotator phase. The effects that changing $c_{p,h}$ and α_h respectively have on the corresponding values of $\mathrm{d}r/\mathrm{d}T$ and $\mathrm{d}u/\mathrm{d}T$ are illustrated in Figure 2. Since α_h is close to 1.7×10^{-3} K^{-1} in most paraffins, as measured by X-ray diffraction,[6,40] it is clear that $\mathrm{d}r/\mathrm{d}T$ significantly exceeds $\mathrm{d}u/\mathrm{d}T$, leading eventually to the observed convergence–divergence change in the p–T diagrams (Figure 1).

The conclusion of the present section can thus be summarized as follows: (a) high heat capacity and thermal expansivity of the hexagonal phase, the necessary prerequisites for its continuous transformation from one (RP) that is close in entropy and volume to the ordered crystal to one (HPHP) that is close to melt, are indeed found experimentally; (b) the collection of published p–T diagrams indicates that the change from convergence of $T_{o-h}(p)$ and $T_{h-m}(p)$, typical of paraffins, to divergence, typical of polyethylene, takes place continuously; (c) measured values for heat capacity and thermal expansivity in a representative paraffin, together with other relevant thermodynamic data, concur with a steep increase in entropy of RP relative to the increase in its volume as the temperature is increased, thus predicting the observed

Table II
Results of the 1306-cm^{-1} IR Band Intensity Measurements

	T, K	A_h/A_m[a]	$c^{T+10}_{GTG,melt}/c^{340}_{GTG,melt}$[b]	c_{kink} (kinks per 100 bonds)[c]
C_{11}	242	0.04	1.1	0.5
C_{23}–C_{25}	307	0.098	1.0	1.1
	318	0.17		1.9
C_{27}[d]	330	0.20	1.00 (ref)	2.3
C_{36}–C_{40}	346	0.20	1.0	2.3
irrad PE	380–400	0.25 ± 0.04	1.1	3.2

[a] Ratio of measured integral absorbance of the 1306-cm^{-1} band in the hexagonal phase and in melt. [b] Ratio of the number of GTG (GTG + GTG*) conformers in molten $(CH_2)_\infty$ at temperature $T + 10$ K and at 340 K, calculated on the basis of the RIS model[48] and assuming a gauche–trans energy difference of 500 cal/mol. [c] Number of kinks per 100 (internal) C–C bonds in the hexagonal phase derived from $c_{kink} = k[c^{T+10}_{GTG,melt}/c^{340}_{GTG,melt}](A_h/A_m)$. Constant k is determined from the data for paraffin C_{27}.[9] [d] From ref 8 and 9.

convergence–divergence change in p–T diagrams.

IR Spectroscopic Results on RP and RIHP

Infrared spectroscopy is particularly suited for evaluating conformational disorder in hydrocarbons. A number of localized defect modes have been identified in IR spectra of linear hydrocarbons, notably in the CH_2 wagging region between 1300 and 1400 cm^{-1}.[8] For example, GTG conformers (GTG and GTG*) appear around 1306 and 1367 cm^{-1}; the band at 1352 cm^{-1} is ascribed to GG defects and that at 1341 cm^{-1} in n-alkane spectra to GT... conformation of the chain end. Contrary to previous views Zerbi and co-workers[7] found that a small proportion of C_{19} molecules have "tilted heads" in the rotator phase, as judged, among other things, by the presence of a weak 1341-cm^{-1} band. Both end-gauche and interior GTG* "kink" defects were observed by Maroncelli, Snyder, and co-workers.[8,9] Within the range of paraffins studied (up to C_{29}) both defect concentrations were found to increase with increasing chain length and, within a single paraffin, with increasing temperature. Evidence for the presence of kinks in RP of longer alkanes has also been provided by the analysis of 00l X-ray diffraction intensities.[4,44]

We have extended a part of the IR study to cover RP in as wide a range of paraffin chain length as is practicable, as well as to RIHP in polyethylene. Only selected results are presented here, while the full account of the IR work will be published separately.[45]

The shortest paraffin studied was C_{11}. For the longest, a mixture of C_{36} and C_{40} (85/15 by weight) was chosen. The reason for mixing the paraffins is that T_{o-h} can thereby be sufficiently lowered with respect to T_{h-m} to enable observation of pure RP free from partial melting. Thus, the addition of C_{40} has lowered T_{o-h} from 73.8 °C for pure C_{36} to 72.7 °C. To minimize the interference of the melt still further, the spectrum analyzed was that of a slightly supercooled RP, recorded at a temperature 0.1 °C above the h–o transition on slow cooling, i.e., at 72.5 °C. The DSC cooling thermogram in Figure 3 shows that no melt is present at this temperature.

As the representative of the paraffins in the intermediate range another binary solid solution, C_{23}–C_{25} (76:24 wt ratio) was selected. In this case the reason for choosing a mixture was the possibility of observing the rotator phase in as wide a temperature range as possible within a single paraffin system,[10] i.e., 15 °C in this case.

Specimens for FTIR spectroscopy were approximately 0.05-mm-thick melt-crystallized paraffins and γ-irradiated polyethylenes, sandwiched between two KBr windows that were separated by appropriate PTFE spacers. The sandwich was held in a variable-temperature cell controlled to within 0.2 K. Four hundred interferograms were coadded for each spectrum by using a Nicolet 7199 instrument with parameters set to give 1-cm^{-1} resolution. Integral band absorbances were obtained by a combination of self-deconvolution and interactive curve fitting.[45]

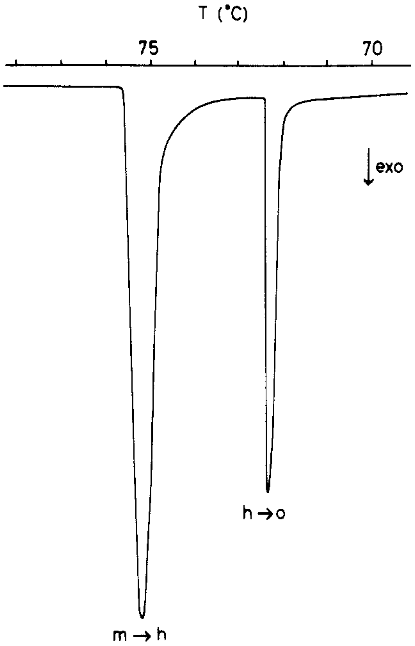

Figure 3. DSC cooling thermogram of the 85/15 (by weight) mixture of n-alkanes C_{36} and C_{40} used in the FTIR experiment. Crystallization and h–o transition exotherms are seen. Cooling rate is 0.62 deg/min.

The ratios of 1306-cm^{-1} band intensities in RP and in the melt, A_h/A_m, are given in Table II for the paraffin systems studied. Like previous authors[8] we consider the 1306-cm^{-1} absorption in RP to be due almost entirely to GTG* kink defects, as GTG conformers are sterically unfeasible in the solid. Very small amounts of GG defects were detected in both solid phases of the mixtures, their presence being attributed mainly to bent chain ends of the longer paraffin component.

The two irradiated polyethylene samples chosen for IR experiments were both melt-crystallized linear Marlex 6002, quenched (q) and slowly cooled (s) from melt, having average X-ray long spacings of 24 and 38 nm, respectively. Samples were γ-irradiated in vacuo at 85 °C with 800 Mrad. The two endotherms in the DSC traces of each sample (Figure 4) correspond to the o–h and h–m transitions, as confirmed by X-ray diffraction. The temperature dependence of the 1306- (GTG) and 1352-cm^{-1} (GG) band intensity is shown in Figure 5 and 6 respectively for both irradiated samples s and q, as well as for unirradiated sample s for comparison.

As can be seen in Figure 5, the GTG defect concentration in both irradiated samples has two regions of steepest ascent with increasing temperature. The temperature of the first corresponds to T_{o-h} and that of the second to T_{h-m}.

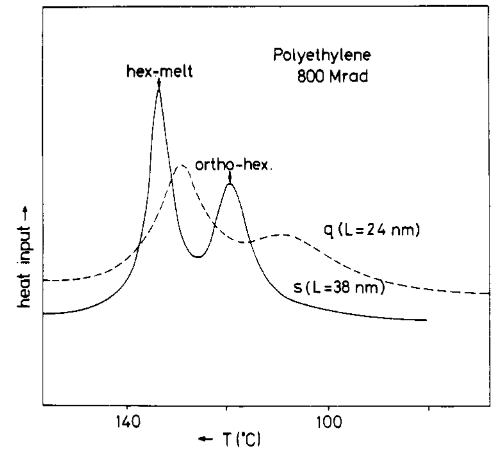

Figure 4. DSC heating thermograms of the two polyethylene samples γ-irradiated with 800 Mrad at 85 °C. X-ray long periods, L, are indicated. Heating rate is 5 deg/min.

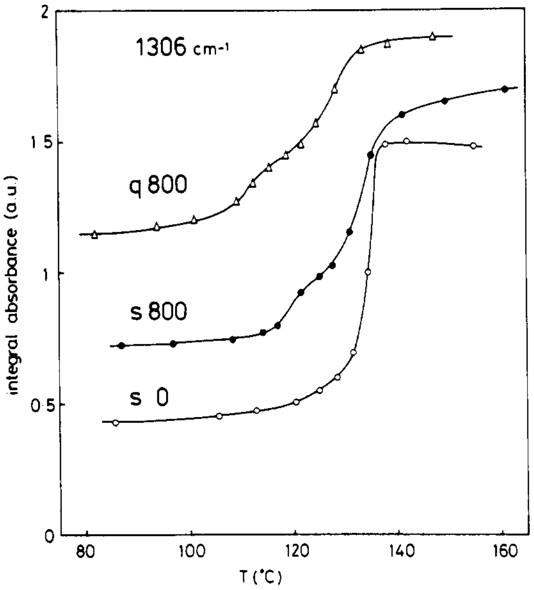

Figure 5. Temperature dependence of the 1306-cm^{-1} GTG* kink band intensity for irradiated polyethylene (samples s and q) and unirradiated sample s. The band was best approximated by two Gaussian components, a major one around 1306 cm^{-1} and a minor one around 1318 cm^{-1}. The curves in the diagrams are normalized to the same intensity in the melt and displaced vertically by 0.2 units for clarity.

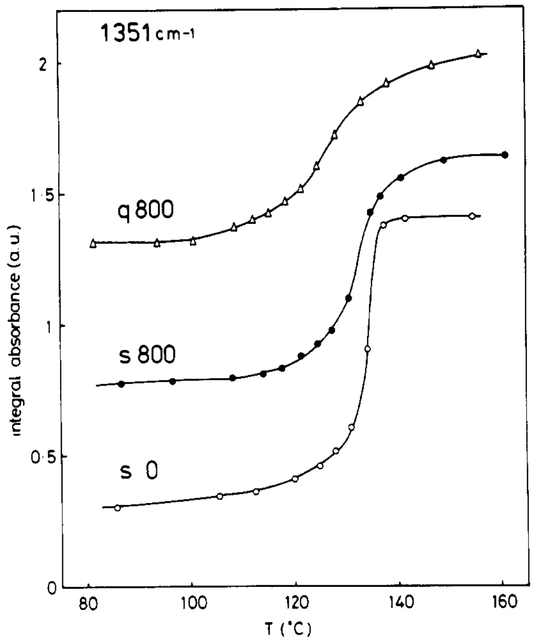

Figure 6. Temperature dependence of the 1352-cm^{-1} GG band intensity for polyethylene samples. The resolved band was approximated by a single mixed Lorentzian-Gaussian profile. Normalization factors are the same as in Figure 5 and the displacement is 0.4 units.

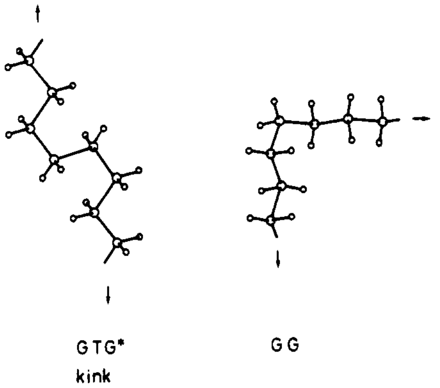

Figure 7. Conformations of a GTG* and a GG defect, adjoined by an all-trans chain on each side.

At the same time the o–h transition does not show up in the GG curves (Figures 6), apart from merely a hint of a shoulder that might even be due to imperfect resolution of the 1352-cm^{-1} band from the nearby GTG band at 1367 cm^{-1}. As with the rotator phase, all increase in the 1306-cm^{-1} band intensity upon the o–h transition is attributed to the formation of GTG* kinks within the crystalline phase. The absence of the sterically improbable GTG defects is among other things supported by the absence of GG defects; both would bend the chain trajectory, while GTG* would not. For comparison Figure 7 illustrates the conformation of GTG* and GG defects.

As solid polyethylene contains an amorphous phase in addition to the crystalline one and as the amorphous content increases somewhat upon irradiation,[46] for the purpose of quantitative analysis we are concerned only with the increases in defect band intensities, above the amorphous base line, that occur upon the o–h and h–m transitions. The height of the o–h step in the 1306-cm^{-1} band intensity is estimated as a quarter of that in the combined (o–h) + (h–m) transition (Figure 5). Thus A_h/A_m is 0.25 in the case of RIHP. The accuracy of this value is limited by some arbitrariness in separating the contribution of the onset of melting from the o–h transition. DSC traces (Figure 4) served as guides in performing the separation.

Absorptivity values are required for determining absolute defect concentrations. Although absorptivity is not explicitly available for the 1306-cm^{-1} band, we can utilize the published data on paraffin C_{27}. The absorbance ratio A_h/A_m for the 1306-cm^{-1} band is reported to be 0.20.[8] A recent independent determination of the G/T ratio for internal bonds in selectively deuterated C_{27} alkanes[9] gave the kink concentration in RP as one in every two molecules, i.e., 2.3 kinks per 100 internal bonds. Here the total GT/TT ratio was measured and the reasonable assumption made that all-gauche internal bonds in RP belong to GTG* kinks. The required absorbtivity ratio was obtained both by group-moment calculation and, independently, by calculating the GT/TT ratio in the melt using the rotational isomeric state (RIS) model.[47]

In order to translate our measured A_h/A_m ratios for the 1306-cm^{-1} band (Table II) into kink concentration in the hexagonal phase (c_{kink}), utilizing the known c_{kink} for C_{27}, we only need account for temperature variation in GTG

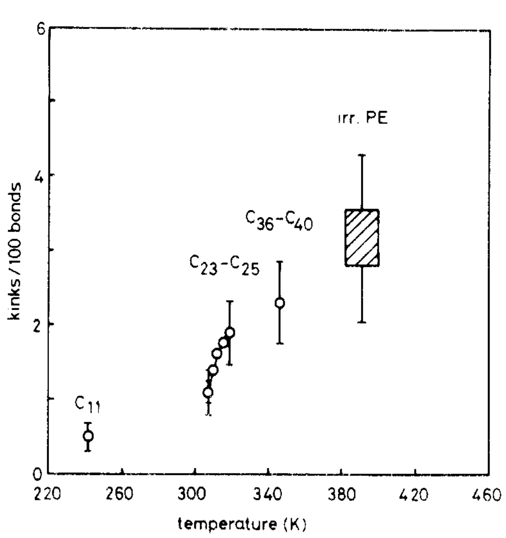

Figure 8. GTG* kink concentration in the rotator phase of alkane C_{11}, binary alkanes C_{23}–C_{25} and C_{36}–C_{40}, as well as in the hexagonal phase of irradiated bulk polyethylene, see Table II. Error bars indicate the estimated absolute error, including that involved in absorptivity calibration. Internal consistency of results is much better: the error in measured absorbance ratios A_h/A_m for paraffins is ±(0.01–0.02).

concentration in the melt. The $c_{\mathrm{GTG,melt}}$ values are calculated for temperatures at which melt spectra were recorded in this work, i.e., approximately 10 °C above the temperatures of the hexagonal phase spectra. The RIS model[48] was applied. The $c_{\mathrm{GTG,melt}}$ values, ratioed against that applicable to paraffin C_{27}, are listed in Table II. In spite of considerable variation in the partition function, GTG concentration in the melt turns out to be fairly constant within the temperature range of interest. Finally, the kink concentrations, derived from the measured A_h/A_m ratios, are listed in the last column of Table II, and plotted against temperature in Figure 8.

Discussion of Spectroscopic Results

The first conclusion derived from the IR experiments is that the types of conformational disorder in RP and RIHP are qualitatively the same; i.e., there are GTG* defects but few, if any, GG defects. In view of the fact that the former leaves the chain direction unaltered, while the latter bends it by 90% (Figure 7), this result comes as no surprise.

Second, it is readily seen from Figure 8 that the steady increase in kink concentration in RP of paraffins, when extended to higher temperature and chain stem length (crystal layer thickness), ties up well with that observed in RIHP. Thus IR experiments show that there is no fundamental discontinuity between RP and RIHP either in the type or in the extent of conformational disorder.

Another feature evident from Figure 8 is that the increase in kink concentration with temperature in a single paraffin system (C_{23}–C_{25}) is much steeper than that between paraffins of different chain lengths. In other words, occurrence of kinks per C atom decreases with increasing chain length, which is consistent with the finding[7,9] that kinks form preferentially near chain ends. Such behavior, i.e., the steep increase in conformational disorder with increasing temperature in RP of a single paraffin, resembles the behavior of the relative entropy/volume ratio discussed in the first part of this paper. This similarity suggests that it is the incorporation of kinks that, at least partly, enables a large gain in entropy with a comparatively low gain in volume of the hexagonal phase in paraffins and polyethylene.

In our previous work[35] the average chain axis periodicity in the hexagonal phase of the same irradiated sample as that used here (sample s, 800 Mrad) has been calculated as 2.46 Å. This value was obtained by combining the *p*–*T* data (specific volume) with the lateral unit cell cross-section derived from X-rays. The chains therefore contract by 3% from the all-trans value of 2.53 Å upon the o–h transition. In the rotational isomeric state approximation one kink shortens the chain by one C–C repeat distance (see Figure 7) and therefore a value of 3 kinks per 100 C atoms is derived for RIHP from *p*–*T* and X-ray data. The present IR result of 3.2 kinks per 100 C atoms thus agrees well with that derived from chain contraction. This agreement is an independent proof of the validity of the adopted procedure for spectroscopic determination of the number of kink defects.

There are no IR data on the high-pressure hexagonal phase in polyethylene so far. Thus, in order to compare the extent of conformational disorder in RP and RIHP with that of HPHP, we rely on the data on percentage chain-axis contraction upon o–h transition. According to most published results, derived from specific volume and lateral lattice parameters, the chains contract by 6–8% upon the transition at temperatures above 500 K.[22] If the contraction is due to kink formation, as has been inferred but not directly proven, this would mean ca. 6–8 kinks per 100 C atoms in HPHP. Thus there appears to be a steady increase in kink concentration in the series: RP(short paraffins) → RP(long paraffins) → RIHP → HPHP. Incidentally, high-pressure IR experiments on HPHP would be highly desirable as they would give more detailed and quantiative information on conformational disorder than is provided by Raman spectroscopy.

Mesophase Observed under Other Conditions and Its General Behavior

The hexagonal phase also occurs in polyethylene fibers containing highly elongated chains if the fiber is heated above the normal melting temperature while the ends are held fixed to prevent retraction.[49] The reduced configurational entropy of constrained melt is clearly responsible for the hexagonal phase being more stable than the melt in this case. High molecular weight cycloalkanes are another group that exhibit a hexagonal or nearly hexagonal high-temperature phase. The low-temperature crystal form contains rings that are collapsed into two parallel straight stems joined by tight folds at each end. In the lower members of the cycloalkane series, $(CH_2)_{22}$ and $(CH_2)_{24}$, the high-temperature phase was found to be highly disordered: (a) the "solid-state" transition involves an entropy 4 times that of final melting,[50] and (b) a kink concentration in the mesophase equal to that in the melt was revealed by spectroscopy.[51] In intermediate-size rings, such as $(CH_2)_{48}$, the solid–solid transition either does not occur or is barely separable from melting.[52] In $(CH_2)_{72}$[53] and $(CH_2)_{92}$[50] the hexagonal phase appears again, but it is less disordered than in the lower cycloalkanes, which seems anomalous at first sight (but see below). From the shape of the IR spectrum of $(CH_2)_{72}$[53] it appears that the kink concentration is comparable to that in our RIHP. Still higher cycloalkanes, up to $(CH_2)_{288}$, have recently all been found to exhibit a mesophase[52] and results of their detailed investigation may be expected in the near future.

In Figure 9 the hexagonal phases occurring in different systems and under different conditions are placed on a temperature vs. $1/n$ map, where n is the number of C atoms in the straight chain stem traversing the crystal layer. As can be seen, the mesophase in cycloalkanes occurs at higher temperatures than that in normal alkanes.

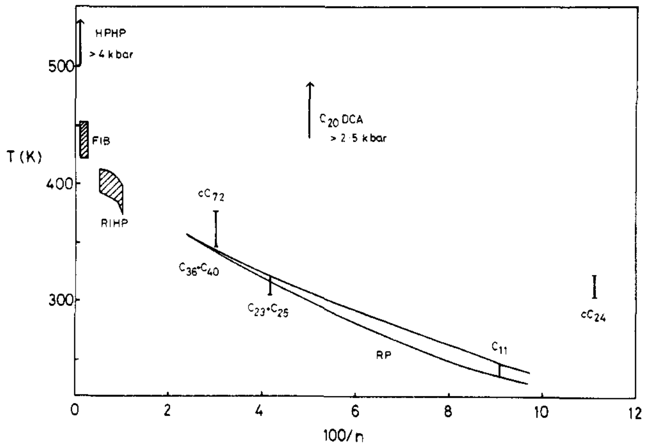

Figure 9. Temperature intervals of stability of the mesophase in different hydrocarbon chain containing systems as a function of the reciprocal number (n) of carbon atoms in the straight stem: RP is the rotator phase in n-alkanes (ref 27 and this work); RIHP is the hexagonal phase in polyethylene irradiated with 800 Mrad (bulk and single crystals); FIB is the gel-spun high-modulus polyethylene fibers under constraint;[49] HPHP is the high-pressure hexagonal phase in chain-extended polyethylene;[22,30] c-C_{24} is cyclotetracosane;[50] c-C_{72} is cyclodoheptacontane;[53] C_{20}DCA is 1,20-eicosanedioic acid under pressure.[36]

In a thermodynamic description a cycloalkane molecule may be regarded as being composed of two n-alkane chains joined at each end. By joining the ends the melting point is increased with respect to that of the n-alkanes due to the disappearance of a Flory–Vrij-type[54] end-unpairing term from the free enthalpy of melting. At the same time this term does not apply to the solid-state transition, the temperature of which is therefore not increased relative to that of the n-alkanes (joining the ends would, however, prevent chain rotation, which is probably the reason for the high hexagonal transition temperature in lower cycloalkanes).

The same thermodynamic argument has also been applied[26] to explain the appearance of the pressure-induced hexagonal phase in 1,20-eicosanedioic acid (C_{20}DCA, see Figure 1). The X-ray diffraction pattern of this mesophase is similar to that of HPHP. The pairing in C_{20}DCA melt is achieved by hydrogen bonding between carboxylic end groups.

Other end-substituted n-alkanes exhibit similar mesophases. Fatty acid monolayers on water[18] and the phospholipid gel phase[17] are closely related to the rotator phase in n-alkanes. The main "chain-melting" transition brings the phospholipid layers into the biologically important smectic state with a high kink concentration.[17]

As a further example, the hexagonal unit cell is observed in certain ethylene–propylene copolymers,[37,40] where a methyl-branch content of about 7 CH_3/100 C atoms raises the free enthalpy of the orthorhombic lattice sufficiently for the hexagonal phase to become stable at room temperature. Introduction of ethyl branches has not been found to produce the hexagonal phase by itself, but it increases the orthorhombic lattice energy sufficiently for the o–h transition to occur at a low irradiation dose.[55]

When all the available information on the hexagonal phase is put together, it appears that all degrees of order intermediate between the highest (RP in paraffin C_{11}) and the lowest (HPHP) are covered in one system or another. Furthermore, it appears that the disorder can be regarded as a continuous function of a few primary variables such as temperature and stem length n. Kink concentration per CH_2 unit, c_{kink}, may be chosen as one of the parameters describing the degree of disorder. Figure 10 is an attempt to depict the qualitative features of such a master function. It has c_{kink} increasing with temperature and decreasing with stem length, as found experimentally. The approximate $c_{\text{kink}} \propto 1/n$ relationship is suggested, e.g., by the fact that in n-alkanes kinks preferentially appear near chain ends.[9] Whenever, in a given system, the free energy of the mesophase becomes the lowest, the phase appears and samples the master relation for a given set of external (e.g., temperature, pressure) and internal (e.g., chain length) variables. Given the limitations of the qualitative approach adopted here, a reasonably coherent pattern emerges of the relationship between the different manifestations of the mesophase. Thus, for instance, in $(CH_2)_{72}$ the phase is similar to that in RIHP according to the similarity in the IR spectra and in the values of lattice cross-section area per chain (A): in $(CH_2)_{77}$ this is 21.1 Å^2,[53] while it is between 21 and 22 Å^2 in our irradiated samples s and q. Likewise, from the X-ray pattern reproduced in ref 49, A can be seen to range from 22 to 23.5 Å^2 in the hexagonal phase of gel-spun polyethylene fibers, indicating a higher disorder than that in RIHP. As to the lower cycloalkanes, $(CH_2)_{22}$ and $(CH_2)_{24}$, they could be considered as more of a special case due to the very small length of stems between the folds (n = 8 and 9, respectively). Nevertheless, the higher disorder in their mesophase compared to that in larger rings, such as $(CH_2)_{72}$, is qualitatively not inconsistent with the present scheme. It is attributed to the fact that in the smaller cycloalkanes the mesophase occurs at temperatures ca. 100 K above that of the rotator phase in corresponding n-alkanes. On the other hand, the hexagonal phase in $(CH_2)_{72}$ becomes stable only 5 K above the melting point of RP in its n-alkane counterpart C_{33}.

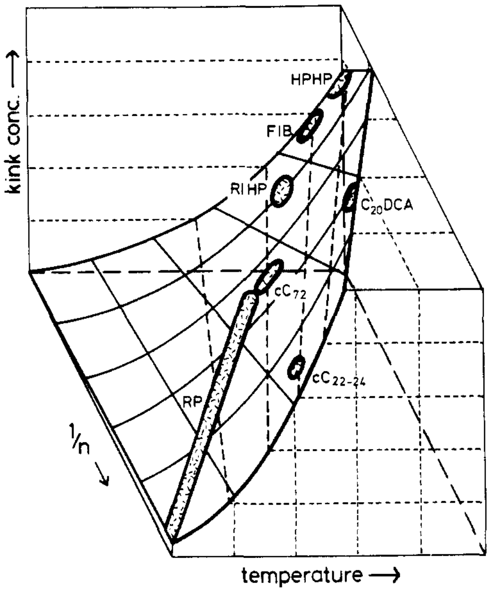

Figure 10. Schematic representation of the extent of conformational disorder in the mesophase as a function of temperature and reciprocal stem length (cf. Figure 9).

It is clear that specific features of individual systems would, to some extent, also affect the degree of order in the mesophase. Thus, irradiation is found to increase the hexagonal lattice cross-section area per chain, A,[31] folds or polar chain ends would prevent rotation of stems, chain-end packing would have some effect, etc. However, it appears that to a good approximation these effects can be treated only as perturbations.

Conclusion

There is abundant evidence, including IR spectroscopic and p–T data, that the rotator phase (RP) in n-alkanes, the high-pressure phase (HPHP) in polyethylene, the radiation-induced hexagonal phase (RIHP) in polyethylene, as well as the hexagonal phase in constrained polyethylene fibers, the high-temperature phase in cycloalkanes and end-substituted *n*-alkanes, etc., are all manifestations of essentially the same mesophase. Its nature appears to vary continuously, covering a very wide range of orientational and conformational disorder. At the low end is the orientationally disordered "rotator" phase in short paraffins, starting with C_{11}: this consists of ordered domains encompassing tens of molecules,[10,16] there are only four equivalent orientations of a chain around its long axis,[10,16] the unit cell is "less hexagonal" (lower a/b ratio) than the ordered orthorhombic one,[6] and there is negligible conformational disorder. At the high end is HPHP with high conformational disorder[30] and an entropy close to that of the melt.[22] The continuity may be attributed to the fact that reorientational jumps of whole stems ("plastic state") *gradually* give way to conformational disorder ("condis state"[29]) in *n*-alkanes as the temperature increases and that a high kink concentration and torsional motion can be tolerated while still maintaining the lateral chain register and considerable lattice energy.

While most theories have so far dealt only with individual mesophase ranges (e.g., either with RP[13-16] or HPHP[24,25]), a more comprehensive treatment should be able to account for the full mesophase range, from the well-ordered plastic paraffins to almost liquidlike polyethylene.

Acknowledgment. Financial support by the Science and Engineering Research Council, UK, and the Science Research Council of Croatia is gratefully acknowledged.

Registry No. $C_{11}H_{24}$, 1120-21-4; $C_{36}H_{74}$, 630-06-8; $C_{40}H_{82}$, 4181-95-7; $C_{23}H_{48}$, 638-67-5; $C_{25}H_{52}$, 629-99-2; polyethylene, 9002-88-4; *n*-heneicosane, 629-94-7.

References and Notes

(1) Müller, A.; *Proc. R. Soc., London, A*, **1932**, *138*, 514.
(2) Barnes, J. D.; Fanconi, B. M. *J. Chem. Phys.* **1972**, *56*, 5190.
(3) Bloor, D.; Bonsor, D. H.; Batchelder, D. H.; Windsor, C. G. *Mol. Phys.* **1977**, *34*, 939.
(4) Strobl, G.; Ewen, B.; Fischer, E. W.; Piesczek, W. *J. Chem. Phys.* **1974**, *61*, 5257.
(5) Doucet, J.; Denicolo, I.; Craievich, A. F.; Germain, C. *J. Chem. Phys.* **1984**, *80*, 1647.
(6) Ungar, G. *J. Phys. Chem.* **1983**, *87*, 689.
(7) Zerbi, G.; Magni, R.; Gussoni, M.; Holland-Moritz, K.; Bigotto, A.; Dirlikov, S. *J. Chem. Phys.* **1981**, *75*, 3175.
(8) Maroncelli, M.; Qi, S. P.; Strauss, H. L.; Snyder, R. G. *J. Am. Chem. Soc.* **1982**, *104*, 6237.
(9) Maroncelli, M.; Strauss, H. L.; Snyder, R. G. *J. Chem. Phys.* **1985**, *82*, 2811.
(10) Ungar, G.; Mašić, N. *J. Phys. Chem.* **1985**, *89*, 1036.
(11) Taylor, M. G.; Kelusky, E. C.; Smith, I. C. P.; Casal, H. L.; Cameron, D. G. *J. Chem. Phys.* **1983**, *78*, 5108.
(12) Doucet, J.; Dianoux, A. J. *J. Chem. Phys.* **1984**, *81*, 5043.
(13) Hoffman, J. D. *J. Chem. Phys.* **1951**, *20*, 541.
(14) Kobayashi, M. *J. Chem. Phys.* **1978**, *68*, 145.
(15) Mazo, M. A.; Oleynik, E. F.; Balabaev, N. K.; Lunevskaya, L. V.; Grivtsov, A. G. *Polym. Bull. (Berlin)* **1984**, *12*, 303.
(16) Yamamoto, T. *J. Chem. Phys.* **1985**, *82*, 3790.
(17) Chapman, D. *Adv. Liq. Cryst.* **1982**, *5*, 1.
(18) Veale, G.; Peterson, I. R. *J. Colloid Interface Sci.* **1985**, *103*, 178.
(19) Bassett, D. C.; Block, S.; Piermarini, G. J. *J. Appl. Phys.* **1974**, *45*, 4146.
(20) Kotov, N.; Zubov, N.; Bakeyev, N. *Dokl. Akad. Nauk SSSR* **1976**, *229*, 1375.
(21) Yamamoto, T. *J. Macromol. Sci.-Phys.* **1979**, *B16*, 487.
(22) Leute U.; Dollhopf, W. *Colloid Polym. Sci.* **1979**, *258*, 353.
(23) Tanaka, H.; Takemura, T. *Polym. J. (Tokyo)* **1980**, *12*, 355.
(24) Priest, R. G. *Macromolecules* **1982**, *15*, 1357; **1985**, *18*, 1504.
(25) Yamamoto, T. *Polymer* **1983**, *24*, 943; **1984**, *25*, 178.
(26) Asahi, T. *J. Polym. Sci., Polym. Phys. Ed.* **1984**, *22*, 175.
(27) Broadhurst, M. G. *J. Res. Natl. Bur. Stand., Sect. A* **1962**, *66A*, 241.
(28) Yasuniva, M.; Enoshita, R.; Takemura, T. *Jpn. J. Appl. Phys.* **1976**, *15*, 1421.
(29) Wunderlich, B.; Grebowicz, J. *Adv. Polym. Sci.* **1984**, *60–61*, 1.
(30) Bassett, D. C. In *Development in Crystalline Polymers* Bassett, D. C., Ed.; Applied Science: London, 1982; Vol. 1, Chapter 2.
(31) Masic, N.; Ungar, G., to be published.
(32) Würflinger, A.; Schneider, G. M. *Ber. Bunsen-Ges. Phys. Chem.* **1973**, *77*, 121.
(33) Fiedler, K. H.; Wunder, S. L.; Priest, R. G.; Schnur, J. M. *J. Chem. Phys.* **1982**, *76*, 5541.
(34) Takamizawa, K.; Sasaki, Y.; Kohno, K.; Urabe, Y.; Ogawa, Y. *Polym. Prepr. Jpn.* **1976**, *25*, 913.
(35) Vaughan, A. S.; Ungar, G.; Bassett, D. C.; Keller, A. *Polymer* **1985**, *26*, 726.
(36) Asahi, T., private communication.
(37) Ungar, G.; Keller, A. *Polymer* **1980**, *21*, 1273.
(38) Keyes, P. H.; Weston, H. T.; Lin, W. J.; Daniels, W. B. *J. Chem. Phys.* **1975**, *63*, 5006.
(39) Shashidhar, R.; Chandrasekhar, S. *J. Phys. Colloq.* **1975**, *36*, 49.
(40) Ungar, G., unpublished.
(41) Pennings, A. J.; Zwijnenburg, A. *J. Polym. Sci., Polym. Phys. Ed.* **1979**, *17*, 1011.
(42) Dollhopf, W.; Grossmann, W. P.; Leute, U. *Colloid Polym. Sci.* **1981**, *259*, 267.
(43) *Landolt-Börnstein Zahlenwerte und Funktionen*, 6th ed.; Springer: Berlin, 1969; Vol. II, Part 4.
(44) Craievich, A. F.; Denicolo, I.; Doucet, J. *Phys. Rev. B: Condens. Matter* **1984**, *30*, 4782.
(45) Ungar, G., in preparation.
(46) Ungar, G. *J. Mater. Sci.* **1981**, *16*, 2635.
(47) Maroncelli, M.; Strauss, H. L.; Snyder, R. G. *J. Phys. Chem.* **1985**, *89*, 4390.
(48) Flory, P. J. *Statistical Mechanics of Chain Molecules*; Interscience: New York, 1969.
(49) Pennings, A. J.; Zwijnenburg, A. *J. Polym. Sci., Polym. Phys. Ed.* **1979**, *17*, 1011.
(50) Grossmann, H. P. *Polym. Bull. (Berlin)* **1981**, *5*, 137.
(51) Grossmann, H. P. *Polym. Bull. (Berlin)* **1982**, *7*, 409.
(52) Lee, K.-S., Doctoral Dissertation; University of Freiburg, Freiburg, West Germany, 1984.
(53) Strobl, G. R.; Schwickert, H.; Trzebiatowski, T. *Ber. Bunsen-Ges Phys. Chem.* **1983**, *87*, 274.
(54) Flory, P. J.; Vrij, A. *J. Am. Chem. Soc.* **1963**, *85*, 3548.
(55) Marks, B. S.; Carr, S. H. *J. Polym. Sci., Polym. Phys. Ed.* **1985**, *23*, 1563.
(56) The term "mesophase" is not restricted here to the liquid-crystalline state. It is used interchangeably with the term "hexagonal phase", which refers to the hexagonal or nearly hexagonal subcell symmetry.[6] Similarly, "orthorhombic" also refers to subcell symmetry.